

Chapter 9

Presynaptic Ca²⁺ Influx and Its Modulation at Auditory Calyceal Terminals

Holger Taschenberger, Kun-Han Lin, and Shuwen Chang

Abstract Calyx and endbulb synapses of the mammalian auditory brainstem are specialized in transmitting spike activity fast, sustained and temporally precise. To accomplish this task, they make use of unusually large presynaptic elements which form axosomatic contacts with their postsynaptic target neurons. The large size of the calyceal terminals represents a major experimental advantage and has enabled electrophysiologists to study the functional properties of Ca²⁺ channels in presynaptic CNS terminals in great detail, with high time resolution and unprecedented precision. Calyx and endbulb terminals express several thousands of Ca²⁺ channels with rapid kinetics which ensure fast and efficient gating of Ca²⁺ influx during brief action potentials. When repetitively activated, presynaptic Ca²⁺ influx is modulated in a frequency-dependent manner and this Ca²⁺ current modulation contributes significantly to short-term plasticity at these synapses. During short high-frequency bursts, Ca²⁺ influx is facilitated whereas tetanic activity or low-frequency firing leads to an accumulation of Ca²⁺ channel inactivation. When the calyx synapses mature, the coupling between docked transmitter vesicles and Ca²⁺ channels becomes tighter to compensate for the shortening of the presynaptic action potential duration. Many of the G protein-dependent pathways of Ca²⁺ channel regulation that are potent in immature synapses are weakened during postnatal development.

Keywords Endbulb of Held • Calyx of Held • Presynaptic function • Presynaptic Ca²⁺ channels • Short-term plasticity

H. Taschenberger (✉) • K.-H. Lin • S. Chang
Research Group Plasticity of Synaptic Transmission, Max Planck Institute for Biophysical Chemistry, 37077 Göttingen, Germany
e-mail: htasche@gwdg.de

9.1 Introduction

Owing to their small size, presynaptic endings of the mammalian brain are generally inaccessible for direct electrophysiological recordings. Thus, our knowledge about the functional properties of presynaptic voltage-gated Ca^{2+} channels (VGCCs) and their regulation is still limited and in many cases has been derived indirectly for example by analyzing postsynaptic responses. Fortunately, there are a few exceptions to this rule. For example, within the mammalian auditory brainstem two glutamatergic axosomatic synapses with exceptionally large presynaptic terminals are found, which have long been known to anatomists for their distinctive and fascinating morphology (Held 1893; Ramón y Cajal 1911; Morest 1968). These are the calyx of Held synapse and its smaller cousin the endbulb of Held synapse. Both synapses participate in sound localization (Masterton et al. 1967) and their structural features appear to facilitate the temporally precise transmission of spike activity along the auditory pathway which is a prerequisite for various tasks of auditory information processing (Rhode and Greenberg 1992; Oertel 1999; Young and Oertel 2004). About 20 years ago, after demonstrating that direct recordings with patch pipettes are feasible at its terminal, calyx of Held synapses—and more recently endbulb synapses too—have been ‘re-discovered’ by electrophysiologists as valuable model for studying presynaptic function (Forsythe 1994; Borst et al. 1995; Lin et al. 2011).

Endbulb and calyx synapses represent the second and third synapses along the binaural auditory pathway. This pathway is involved in computing sound source localization in the auditory space by detecting interaural timing and level differences of sound and synapses participating in this task are specialized for transmitting electrical signals fast and reliably. Endbulb synapses are formed between the endings of auditory nerve fibers and bushy cells (BCs) in the anterior ventral cochlear nucleus (AVCN). The axons of spiral ganglion cells convey auditory sensory information from the inner hair cells to spherical BCs (SBCs) via large calyx-type axosomatic terminals—the endbulbs of Held. SBCs carry timing information to the medial superior olivary nuclei, where the arrival time of sounds at the two ears is compared. Detailed reconstructions of endbulb → SBC connections have revealed that up to four endbulb terminals can contact single bushy cells (Fig. 9.1b) (Brawer and Morest 1975; Ryugo and Sento 1991; Nicol and Walmsley 2002). Each endbulb terminal can harbor many active zones with large clusters of synaptic vesicles (Neises et al. 1982; Ryugo et al. 1996, 1997; Nicol and Walmsley 2002).

The calyx of Held synapse is formed by fibers originating from the globular bushy cells (GBCs) of the AVCN and terminating onto principal cells of the medial nucleus of the trapezoid body (MNTB) which is situated ventromedial to the medial superior olive (MSO). Each principal neuron is contacted by only a single presynaptic fiber that ends in the form of a cup-like termination—the calyx of Held—which embraces approximately two thirds of the principal cell’s membrane surface (Fig. 9.1a) (Morest 1968). Among glutamatergic synapses of the mammalian brain, the calyx of Held has without a doubt become one of the

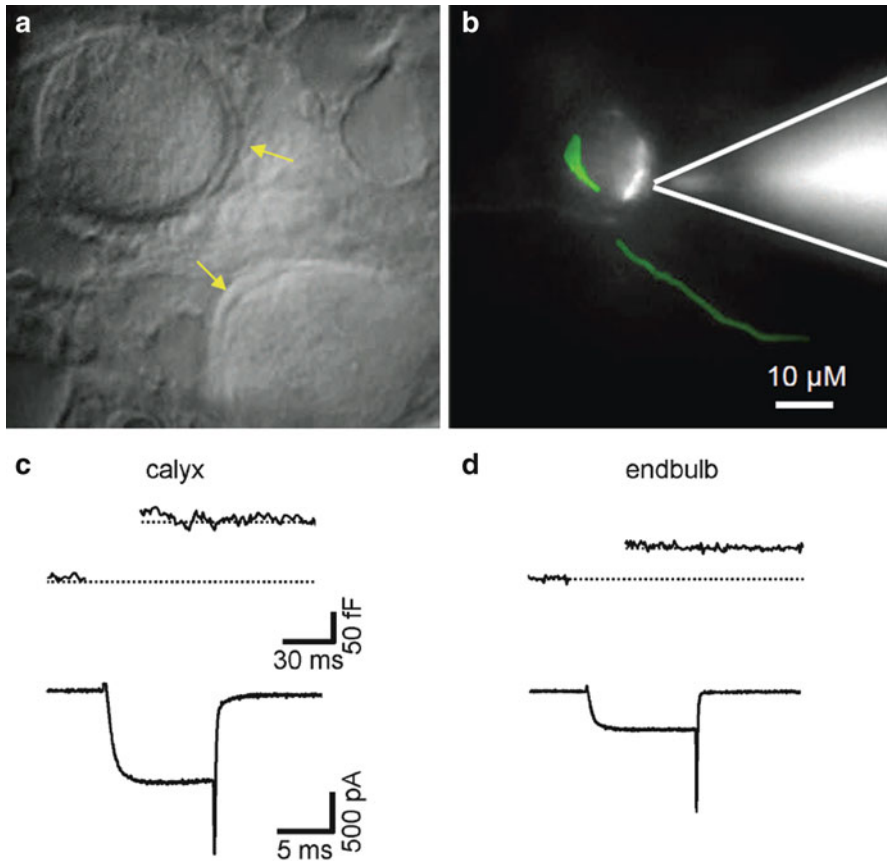


Fig. 9.1 Identification of calyx and endbulb terminals. Two hundred μm thick slices were prepared from brainstems of a postnatal day 9 rat (a) or mouse (b). (a) MNTB principal neurons visualized using differential interference contrast. Each principal cell is surrounded by a single giant presynaptic terminal—the calyx of Held (arrows). (b) Bushy cells of the anterior ventral cochlear nucleus (AVCN) are contact by several large endbulb terminals. Here, two terminals contacting a single bushy cell were sequentially loaded with a fluorescent dye via a presynaptic patch pipette (white lines). (c, d) Changes in membrane capacitance (ΔC_m , top) elicited by step-depolarizations (10 ms, from $V_h = -80$ to 0 mV) recorded from a calyx (b) and an endbulb (d) terminal. The corresponding $I_{\text{Ca(V)}}$ are shown in the bottom panel

best characterized (for review see Schneggenburger et al. 2002; von Gersdorff and Borst 2002; Meinrenken et al. 2003; Schneggenburger and Forsythe 2006; Borst and Soria van Hoeve 2012). This derives primarily from the unusual large size of its presynaptic terminal which, therefore, renders it accessible to patch pipettes (Forsythe 1994; Borst et al. 1995; Takahashi et al. 1996; Chuhma and Ohmori 1998; Sun and Wu 2001). Because of its giant size, the calyx terminal harbors several hundreds of release sites, allowing it to drive the principal neurons reliably at

high frequencies. The principal neurons of the MNTB are glycinergic and provide precisely timed and sustained inhibition to many other auditory brainstem nuclei. The calyx of Held synapse thus functions as a fast, reliable, inverting relay synapse.

9.2 General Characteristics, Number and Distribution of Presynaptic VGCCs

During patch-clamp experiments in brainstem slices, endbulb and calyx terminals are easily identifiable (Fig. 9.1a, b) and the presynaptic origin of the recordings can conveniently and unequivocally be verified by monitoring transmitter release after depolarization-induced Ca^{2+} influx. The fusion of transmitter vesicles leads to an transient increase in membrane area, which can be measured as an increase in surface membrane capacitance (Jaffe et al. 1978; Gillespie 1979; Neher and Marty 1982; Lin et al. 2011) (Fig. 9.1c, d). When pharmacologically isolated, inward whole-cell Ca^{2+} currents ($I_{\text{Ca}(\text{V})}$) with peak amplitudes typically between 0.5 and 2.5 nA can be recorded in mouse or rat calyx of Held terminals with 2 mM external Ca^{2+} (Borst et al. 1995; Borst and Sakmann 1996, 1998b; Chuhma and Ohmori 1998; Forsythe et al. 1998). The presynaptic $I_{\text{Ca}(\text{V})}$ appears to be relative resistant to run-down after internal dialysis has begun, at least in the presence of internal ATP and ATP-regenerating substrates such as phosphocreatine. The average $I_{\text{Ca}(\text{V})}$ in endbulb terminals is about two thirds smaller than that of the calyx which is consistent with the much smaller size of the endbulb terminals (Lin et al. 2011) (Fig. 9.1 c, d). Despite the considerable variability of $I_{\text{Ca}(\text{V})}$ amplitudes among individual calyx and endbulb terminals, a relatively robust linear correlation between $I_{\text{Ca}(\text{V})}$ and the membrane capacitance is observed indicating a rather similar average current density of ~ 0.076 nA/pF and ~ 0.1 nA/pF in calyx and endbulb terminals, respectively (Fig. 9.2) (Lin et al. 2011). The presynaptic $I_{\text{Ca}(\text{V})}$ shows the typical bell-shaped I-V relationship: it activates at membrane potentials more positive than -40 mV and peaks between -10 and 0 mV. The presynaptic Ca^{2+} channels show remarkably little steady state inactivation (Fig. 9.3) (Forsythe et al. 1998; Lin et al. 2011) and, in contrast to the bushy cell bodies, neither calyx nor endbulb terminals express low-voltage activated, transient (T-type) Ca^{2+} currents. One may argue that failsafe transmission at these synapses requires relative insensitivity to fluctuations of the presynaptic resting membrane potential, and T-type Ca^{2+} channels would be especially ill-suited for the purpose of triggering action potential-evoked presynaptic Ca^{2+} influx reliably.

Noise analysis of $I_{\text{Ca}(\text{V})}$ amplitude fluctuations provided estimates for the apparent single channel current of ~ 0.08 pA at a membrane potential of 0 mV, suggesting that on average $>6,000$ and $>16,000$ open channels contribute to generating average current amplitudes of 0.5 and 1.3 nA in endbulb and calyx terminals, respectively (Lin et al. 2011). These single channel current estimates are slightly smaller than those obtained at hippocampal mossy fiber boutons (0.13 pA

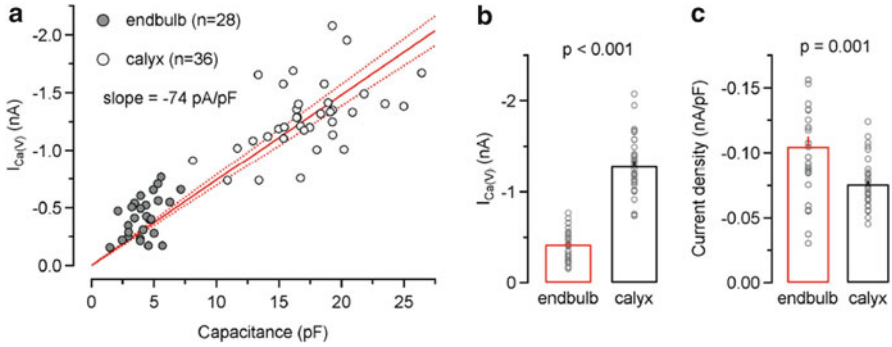
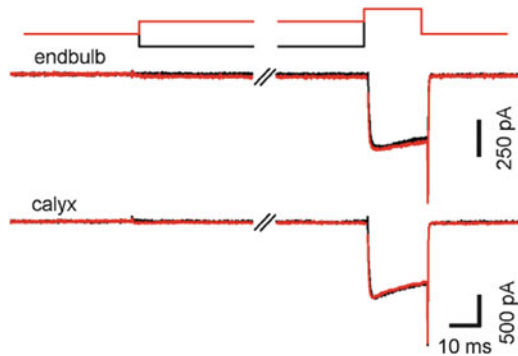


Fig. 9.2 Ca²⁺ current densities are slightly larger in endbulb versus calyx terminals. **(a)** Scatter plot of $I_{Ca(V)}$ versus terminal capacitance obtained from 28 endbulb and 36 calyx terminals. *Solid and dotted red lines* represent linear regression and 95 % confidence intervals for the entire data set, respectively. The slope of the regression line is -74 pA/pF. **(b, c)** Average amplitudes **(b)** and current densities **(c)** of $I_{Ca(V)}$ in endbulb and calyx terminals (Modified from Lin et al. 2011)

Fig. 9.3 Negligible steady-state inactivation of $I_{Ca(V)}$. $I_{Ca(V)}$ was elicited in endbulb (*middle traces*) and calyx (*bottom traces*) terminals by 20 ms pulses to 0 mV after conditioning depolarization (500 ms duration) to -120 mV (black) or -40 mV (*top traces*) (Modified from Lin et al. 2011)



at 0 mV) (Li et al. 2007). Using slightly elevated external Ca²⁺ (10 mM), larger single channel currents (0.27 pA) were measured recently by directly recording in the cell-attached configuration from the terminal’s release face that was exposed by applying positive pressure in brainstem slices pretreated with the protease papain (Sheng et al. 2012). Nevertheless, it is conceivable that single endbulb and calyx terminals harbor several thousands of VGCCs.

How are these channels distributed over the presynaptic membrane? Whilst ultra-structural data is still missing, some insights about the spatial organization of Ca²⁺ channels can be gained from dual patch-clamp recordings at the calyx of Held. When monitoring transmitter release after direct presynaptic depolarizations with voltage commands that cause the opening of a variable number of Ca²⁺ channels, the EPSC size changes in a supralinear manner. It was therefore concluded that the majority of readily releasable vesicles at the calyx is controlled by several Ca²⁺ channels per vesicle (Borst and Sakmann 1999). This contrasts the situation at

the squid giant synapse (Augustine et al. 1991), the frog neuromuscular junction (Yoshikami et al. 1989) and the chick ciliary ganglion synapse (Stanley 1993), where the release of synaptic vesicles seems to be controlled by only a single Ca^{2+} channel. Assuming that the vast majority of Ca^{2+} channels are concentrated at active zones and considering the total number of readily releasable vesicles in endbulb and calyx synapses, one arrives at an estimate of approximately 6–8 VGCCs that are associated with each docked vesicle (Lin et al. 2011). Cell-attached patch recordings from the release face of calyx terminals revealed that single active zones contain an average number of ~ 40 VGCCs (Sheng et al. 2012). No Ca^{2+} currents are detected in patches from the calyx membrane not opposed to the postsynaptic neuron reinforcing the notion that VGCCs must be clustered at the release face (Sheng et al. 2012).

Immature calyces of Held (\leq postnatal day (P) 12) express a mixture of N-, R-, and P/Q-type Ca^{2+} channels among which P/Q-type channels couple more efficiently to release than the other types do, suggesting that they are more concentrated at active zones (Wu et al. 1999). In contrast, endbulb terminals nearly exclusively express Ca^{2+} channels of the P/Q-type (Lin et al. 2011). The same applies for calyces of post-hearing mice and rats suggesting a developmental shift in the expression of their α -subunits (see below) (Iwasaki and Takahashi 1998; Iwasaki et al. 2000).

9.3 Ca^{2+} Influx During Presynaptic Action Potentials

Borst and Sakmann (1998b) measured the presynaptic $I_{\text{Ca}(\text{V})}$ during an action potential (AP) waveform using two-electrode voltage-clamp at juvenile (P 8–10) rat calyces. These experiments revealed important information about magnitude and timing of the presynaptic Ca^{2+} influx in a mammalian CNS terminal. The AP-evoked $I_{\text{Ca}(\text{V})}$ starts shortly after the peak of the calyceal AP and ends before the terminal is fully repolarized. This leads to a rapid rise in the global intracellular free Ca^{2+} ($[\text{Ca}^{2+}]_i$) with a rise time of ~ 0.32 ms (Habets and Borst 2006). The rapid gating kinetics of Ca^{2+} channels in the calyx of Held allows the AP to open the channels quite effectively such that the peak $I_{\text{Ca}(\text{V})}$ during the AP repolarization phase is ~ 70 % of its maximum possible size. The AP-driven $I_{\text{Ca}(\text{V})}$ can be well described by a Gaussian function having a peak amplitude of about -2.5 nA and a half-width of ~ 0.36 ms. The current integral is about -0.92 pC (Borst and Sakmann 1998b). At near physiological temperature, peak amplitudes almost double compared to recordings obtained at room temperature. However, because the AP half-width decreases by approximately 50 % when raising temperature, the total Ca^{2+} influx is actually smaller at near physiological compared with room temperature.

Endbulb APs are slightly smaller in amplitude and shorter in duration compared to calyx APs and thus open presynaptic Ca^{2+} channels less effectively. Because of their much smaller size, two-electrode voltage-clamp is not feasible at endbulb

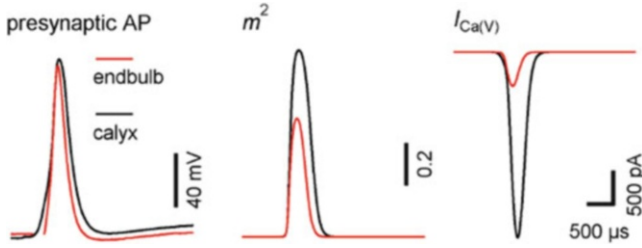


Fig. 9.4 Comparison of simulated $I_{\text{Ca(V)}}$ during presynaptic endbulb and calyx APs. *Left*, Endbulb APs (black) are slightly smaller in amplitude and shorter in duration compared to those recorded from calyces (gray). V_m was -80 mV. *Middle*, Simulated time course of the activation parameter m^2 . Because of its larger amplitude and longer duration, the calyceal AP waveform opens presynaptic VGCCs more efficiently than the endbulb AP. *Right*, Simulated $I_{\text{Ca(V)}}$ during presynaptic APs in endbulb (black) and calyx (gray). On average, the simulated presynaptic $I_{\text{Ca(V)}}$ is ~ 6 times smaller for endbulb compared to calyx terminals (Modified from Lin et al. 2011)

terminals. Using the Hodgkin-Huxley formalism to model AP-driven Ca^{2+} influx, it was shown that the open probability (m^2 activation parameter) peaks at a considerably lower value in endbulb (0.49) compared to calyx (0.88) terminals of mice of the same age, even though the Ca^{2+} channel gating kinetics is of similar speed in both types of terminals (Lin et al. 2011). Together with the much lower number of Ca^{2+} channels expressed in endbulb terminals this results in a simulated $I_{\text{Ca(V)}}$ of comparably rapid kinetics but with ~ 6 times smaller amplitude (-0.45 vs. -2.8 nA; Fig. 9.4) (Lin et al. 2011).

9.4 Inactivation of Presynaptic VGCCs

During prolonged presynaptic depolarizations, $I_{\text{Ca(V)}}$ inactivates with a double-exponential time course (Forsythe et al. 1998; Lin et al. 2012). The fast component of inactivation has a time constant of ~ 35 ms and appears to be Ca^{2+} -dependent as it is greatly reduced when Ca^{2+} is replaced by Ba^{2+} in the external ringer solution, whereas the slow component of inactivation is largely unchanged (Lin et al. 2012). A plot of $I_{\text{Ca(V)}}$ inactivation following conditioning voltage pulses against membrane potential shows an inverse bell-shaped curve mirroring the I-V relationship which further suggests that inactivation is caused by Ca^{2+} influx (Forsythe et al. 1998). The Ca^{2+} sensor for Ca^{2+} -dependent inactivation must be pre-associated with the channel itself because, similarly to what is observed in dorsal root ganglion neurons (Morad et al. 1988), the onset of current activation after UV-flash photolysis of caged Ca^{2+} is virtually instantaneous at the calyx of Held (Fig. 9.5) (Lin et al. 2012).

Approximately 45 % of $I_{\text{Ca(V)}}$ inactivates during 100 ms step depolarizations. This fractional inactivation is remarkably insensitive to manipulations of the

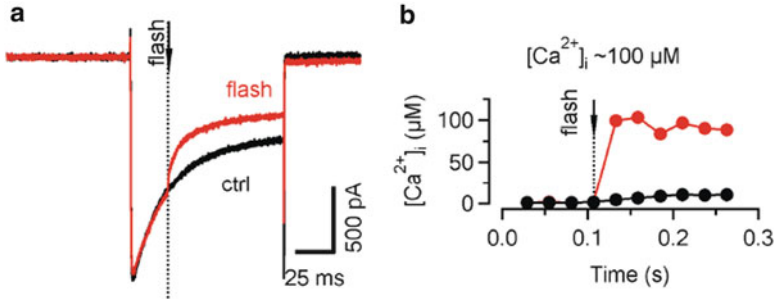


Fig. 9.5 Onset kinetics of Ca^{2+} -dependent inactivation after flash photolysis of caged Ca^{2+} . $I_{\text{Ca(V)}}$ (a) elicited by step depolarizations to 0 mV with (red) and without (black) a UV-light flash (dotted line) delivered ~ 25 ms after current onset. Corresponding changes in $[\text{Ca}^{2+}]_i$ are illustrated in (b). The post flash $[\text{Ca}^{2+}]_i$ increased to ~ 100 μM . Note the immediate acceleration of the inactivation time course after Ca^{2+} uncaging (Modified from Lin et al. 2012)

intracellular Ca^{2+} buffering strength as it is virtually unchanged when replacing 0.5 mM EGTA by 30 mM BAPTA in the pipette solution. If Ca^{2+} channels are clustered at the active zone (Roberts et al. 1990; Llinas et al. 1992; Westenbroek et al. 1995; DiGregorio et al. 1999; Harlow et al. 2001; Nagwaney et al. 2009), high concentrations of Ca^{2+} are also reached in between channels and the local $[\text{Ca}^{2+}]_i$ transient built-up by the overlapping Ca^{2+} domains within such channel clusters may be difficult to buffer effectively. This may explain why lowering the density of functional Ca^{2+} channels by application of the open-channel blocker ω -AgaTx quite effectively reduces the amount of inactivation during voltage steps. In contrast, reducing Ca^{2+} influx to a similar extent by means of lowering the external Ca^{2+} concentration does not affect inactivation significantly (Lin et al. 2012).

The $[\text{Ca}^{2+}]_i$ requirements for inducing Ca^{2+} -dependent inactivation can be directly assayed using flash photolysis-induced Ca^{2+} uncaging (Lin et al. 2012). Using such approach, the amount of $I_{\text{Ca(V)}}$ inactivation after step-like UV flash-induced elevations of $[\text{Ca}^{2+}]_i$ to various levels can be quantified. Inactivation starts to occur at elevations of $[\text{Ca}^{2+}]_i > 2$ μM and reaches a plateau at ~ 100 μM . Half-maximum inactivation is measured at ~ 6 μM . For comparison, a single presynaptic AP elevates $[\text{Ca}^{2+}]_i$ by only ~ 400 nM (Helmchen et al. 1997; Müller et al. 2007) but during repetitive AP firing at high-frequency the level of free intracellular Ca^{2+} can reach several micromoles (Billups and Forsythe 2002; Korogod et al. 2005; Müller et al. 2007). Thus, it is likely that Ca^{2+} -dependent inactivation in intact terminals is most effectively induced by AP trains (see below). Ca^{2+} -dependent inactivation of calyceal $I_{\text{Ca(V)}}$ depends on the interaction of the channels with calmodulin as it is attenuated by pre-incubating slices with the calmodulin antagonist calmidazolium or intraterminal application of myosin light chain kinase (MLCK) peptide, a specific inhibitor of calmodulin (Xu and Wu 2005; Nakamura et al. 2008).

9.5 Recovery from Inactivation

When $I_{\text{Ca(V)}}$ inactivation is induced with very long depolarizations (1.9 s), complete recovery takes more than 1 min. The recovery has a bi-exponential time course with fast and slow time constants of ~ 7.5 s and 50 s, respectively, and the fast component accounting for about two thirds of the recovery (Forsythe et al. 1998). Presumably, after such prolonged periods of Ca^{2+} influx that are likely to saturate cytosolic Ca^{2+} buffers, the delayed clearance of Ca^{2+} from the cytoplasm may contribute to the very slow recovery from inactivation. After shorter voltage steps (100 ms), Ca^{2+} channels recover much more quickly from inactivation with fast and slow time constants of ~ 0.2 s and 5 s, respectively, and the fast component contributing about 75 % (Fig. 9.6) (Lin et al. 2012).

During step depolarizations under typical whole-cell recording conditions (0.5 mM EGTA), the global volume-averaged $[\text{Ca}^{2+}]_i$ can reach peak amplitudes of several micromoles and slowly decays back to its resting level with a bi-exponential time course. However, the time course of recovery from Ca^{2+} channel inactivation seems to be unrelated to the Ca^{2+} clearance time course but rather reflects intrinsic channel properties as it is unchanged even when $[\text{Ca}^{2+}]_i$ is strongly buffered by including 10 mM EGTA or BAPTA in the pipette solution, a manipulation which nearly completely suppresses the slowly decaying residual Ca^{2+} transient after step depolarizations (Fig. 9.6) (Lin et al. 2012). The slow recovery from inactivation allows accumulation of Ca^{2+} channel inactivation during repetitive channel gating such as during AP trains (see below).

9.6 Facilitation of Presynaptic VGCCs

Following pre-depolarizations, calcium channels gating is accelerated (Borst and Sakmann 1998a; Cuttle et al. 1998). Using paired-pulse protocols of short, 1 ms voltage steps to -10 mV, $I_{\text{Ca(V)}}$ is facilitated for inter-pulse intervals ≤ 100 ms. The facilitation is greater at shorter intervals with a maximum of about 20 % for intervals of 5–10 ms (Cuttle et al. 1998). The facilitation of $I_{\text{Ca(V)}}$ can be explained by an acceleration of the voltage-dependent rate constant (α_m) for opening which produces a hyperpolarizing shift in the I-V relationship of about -4 mV (Borst and Sakmann 1998a; Cuttle et al. 1998). The faster opening of the facilitated channel is particularly evident during steps to slightly more negative membrane potentials between -25 and 15 mV at which the activation rate of non-facilitated Ca^{2+} channels is relatively slow (Fig. 9.7).

It is conceivable that $I_{\text{Ca(V)}}$ may be tonically suppressed by presynaptic G protein-coupled receptors and relief from this suppression may cause facilitation. However, experiments using $\text{GTP}\gamma\text{S}$ and $\text{GDP}\beta\text{S}$ rule out an involvement of G protein-coupled mechanisms (Cuttle et al. 1998). $I_{\text{Ca(V)}}$ facilitation is also unaffected by intense hyperpolarization following the conditioning pulse (Cuttle et al. 1998;

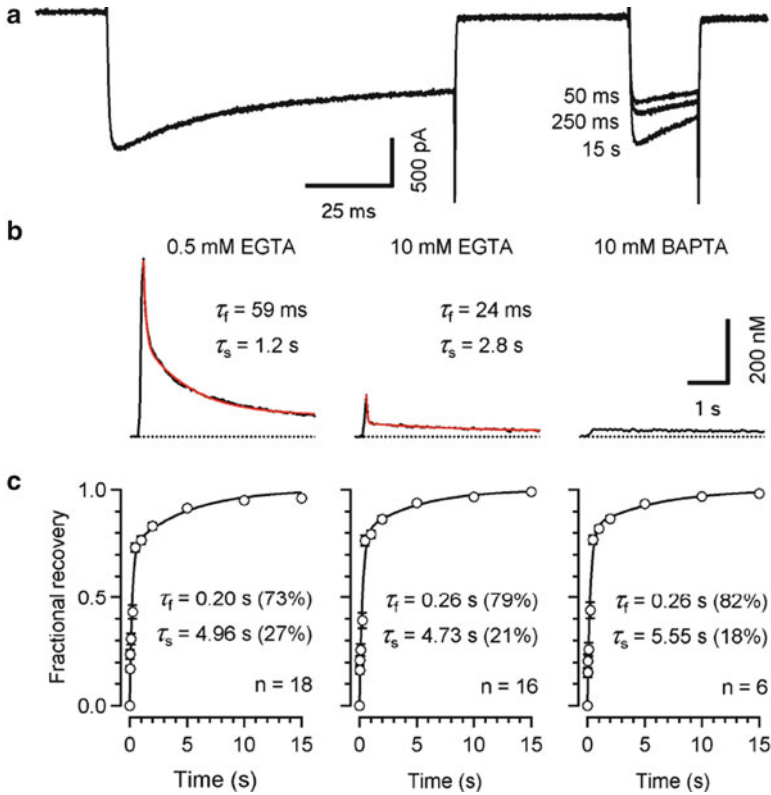


Fig. 9.6 Recovery of $I_{Ca(V)}$ from inactivation is slow. **(a)** Recovery of $I_{Ca(V)}$ from inactivation tested at variable intervals using a paired-pulse protocol consisting of a 100 ms depolarization to 0 mV followed by a 20 ms depolarization to 0 mV at variable inter-stimulus interval. Pipette solution contained 0.5 mM EGTA. Traces for three different recovery intervals are shown superimposed. **(b, c)** The time course of recovery from inactivation is biphasic and insensitive to changes in Ca^{2+} buffer strength. **(b)** $[Ca^{2+}]_i$ transients evoked by 100 ms step depolarizations. The rise of global $[Ca^{2+}]_i$ is nearly completely suppressed when adding 10 mM BAPTA to the pipette solution (*right panel*). **(c)** Average time course of recovery from inactivation. *Solid lines* represent double exponential fits. Fast and slow time constants were similar for the three $[Ca^{2+}]_i$ buffering conditions. Relative amplitudes of fast and slow time constants are given in *parenthesis* (Modified from Lin et al. 2012)

Lin et al. 2012), arguing against a contribution of voltage. Rather, it depends on the build-up of intracellular Ca^{2+} , because its magnitude is proportional to the Ca^{2+} influx (Borst and Sakmann 1998a; Cuttle et al. 1998) and it is abolished when substituting external Ca^{2+} with Ba^{2+} (Fig. 9.7a, b) (Cuttle et al. 1998; Lin et al. 2012). High concentrations (≥ 10 mM) of the fast Ca^{2+} buffer BAPTA reduce the amount of facilitation of the peak $I_{Ca(V)}$ elicited by action potential waveforms (Borst and Sakmann 1998a) or short AP-like voltage steps whereas the slow buffer EGTA is much less effective (Cuttle et al. 1998). On the other hand,

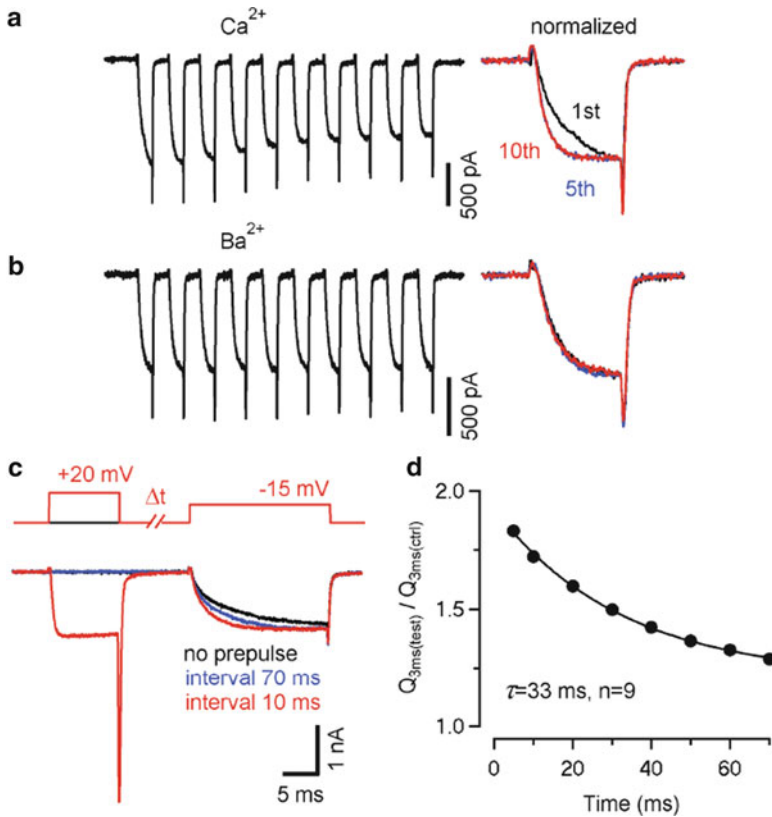


Fig. 9.7 Ca^{2+} dependent facilitation of $I_{\text{Ca}(V)}$ during pre-pulse protocols. **(a, b)** $I_{\text{Ca}(V)}$ elicited by a 100 Hz train of 5 ms steps from $V_h = -80$ mV to -20 mV in P8 calyces. **(a)** With Ca^{2+} as the charge carrier (the activation of $I_{\text{Ca}(V)}$ strongly accelerated from the first to the fifth voltage step and remained fast during later steps. **(b)** No change in activation kinetics was observed with external Ba^{2+} . *Right panel:* first, fifth and tenth $I_{\text{Ca}(V)}$ shown superimposed for comparison after normalizing to the same peak amplitude. **(c)** Sample traces of $I_{\text{Ca}(V)}$ without (black trace) or with prepulse at 10 ms (red) or 70 ms interval (blue). **(d)** The relaxation of $I_{\text{Ca}(V)}$ facilitation is an order of magnitude faster than recovery from inactivation. *Solid line* represent single exponential fit with a decay time constant as indicated (Modified from Lin et al. 2012)

when facilitation is assayed as increase in charge transfer during the initial 3 ms of $I_{\text{Ca}(V)}$ elicited by voltage steps to -20 or -15 mV, including either 10 mM EGTA or 10 mM BAPTA reduces facilitation only slightly (Lin et al. 2012). The relaxation of $I_{\text{Ca}(V)}$ facilitation follows an exponential time course with a time constant of ~ 30 ms (Fig. 9.7c, d) (Cuttle et al. 1998; Lin et al. 2012) and is thus about an order of magnitude faster than the recovery from current inactivation. Therefore, accumulation of Ca^{2+} channel facilitation during repetitive activation of $I_{\text{Ca}(V)}$ is more restricted and can only occur at very short inter-stimulus intervals.

UV-flash photolysis-evoked Ca^{2+} uncaging elicits $I_{\text{Ca(V)}}$ facilitation of similar magnitude compared to that evoked by voltage pre-pulses (Lin et al. 2012). In such experiments, elevation of $[\text{Ca}^{2+}]_i > 1 \mu\text{M}$ are required to induce appreciable $I_{\text{Ca(V)}}$ facilitation and concentrations $> 20 \mu\text{M}$ do not further increase the amount of facilitation. However, the magnitude of facilitation is generally small and, especially at high Ca^{2+} concentrations, it is difficult to separate facilitation from inactivation which makes establishing a dose-response relationship between $[\text{Ca}^{2+}]_i$ and $I_{\text{Ca(V)}}$ facilitation more complicated. Nevertheless, it appears as if the $[\text{Ca}^{2+}]_i$ requirements for inducing $I_{\text{Ca(V)}}$ facilitation and inactivation are rather similar. The facilitation of Ca^{2+} currents seems to depend largely on an interaction with the high-affinity calcium-binding protein neuronal calcium sensor 1 (NCS-1). Direct loading of NCS-1 into calyx terminals mimics and partially occludes Ca^{2+} -dependent facilitation of $I_{\text{Ca(V)}}$ (Tsujiimoto et al. 2002). On the other hand, $I_{\text{Ca(V)}}$ facilitation during trains of very high frequencies (500 Hz) is also sensitive to inhibition of calmodulin, suggesting an additional Ca^{2+} channel-calmodulin interaction (Nakamura et al. 2008).

9.7 Modulation by G Protein-Coupled Receptors

Calyx of Held synapses expresses presynaptic group II and III metabotropic glutamate receptors (mGluRs) that are negatively coupled to neurotransmitter release (Barnes-Davies and Forsythe 1995; Takahashi et al. 1996; von Gersdorff et al. 1997). In addition to mGluR agonists, GABA_B receptor, $\alpha 2$ -adrenoreceptor, 5-HT receptor and A₁ receptor agonists can presynaptically attenuate synaptic transmission (Barnes-Davies and Forsythe 1995; Leao and von Gersdorff 2002; Kimura et al. 2003; Mizutani et al. 2006). Baclofen, L-AP4, 5-HT, adenosine and noradrenaline inhibit the presynaptic $I_{\text{Ca(V)}}$ without affecting K⁺ currents or AP-waveform, and their inhibitory effect on EPSCs can be fully explained by the reduction in Ca^{2+} influx (Takahashi et al. 1996, 1998; Leao and von Gersdorff 2002; Kimura et al. 2003; Mizutani et al. 2006). A₁ receptors share a common mechanism for the presynaptic inhibition with GABA_B receptors because in the presence of baclofen, adenosine no longer attenuates EPSCs (Kimura et al. 2003). Similarly, L-AP4 occludes the inhibition by noradrenaline of EPSCs when applied first. However, mGluRs are more potent modulators of $I_{\text{Ca(V)}}$ because after inhibition by noradrenaline, L-AP4 is able to further inhibit the Ca^{2+} current (Leao and von Gersdorff 2002). In contrast to its inhibitory effect at the calyx of Held, noradrenaline potentiates the size of EPSCs at another calyx-type synapse in the chick ciliary ganglion and this is due to a cGMP-dependent mechanism that increases the Ca^{2+} sensitivity of exocytosis (Yawo 1999).

What are the endogenous agonists for the modulation of $I_{\text{Ca(V)}}$ by G protein-coupled receptors? Obviously, synaptically released glutamate can induce feedback inhibition via mGlu autoreceptor activation. In fact, mGluR antagonists attenuate steady state depression of EPSCs during train stimulation (von Gersdorff et al. 1997;

Iwasaki and Takahashi 2001). Endogenous adenosine seems to be co-released during presynaptic AP firing, because application of the A_1 antagonist CPT slightly but significantly increases the steady-state EPSC amplitude during 10 Hz trains (Kimura et al. 2003). The MNTB also receives adrenergic input (Jones and Friedman 1983; Wynne and Robertson 1996). However, the physiological function of this adrenergic innervation is not well understood. Alternatively and/or additionally, the ambient concentrations of GABA, glutamate, adenosine or noradrenalin may provide tonic inhibition of $I_{\text{Ca(V)}}$ (Cavelier et al. 2005; Glykys and Mody 2007).

9.8 Modulation of Presynaptic Ca^{2+} Influx During AP-Like Stimulus Trains

The regulation of AP-driven Ca^{2+} influx represents a powerful mechanism to modulate synaptic strength because transmitter release is highly nonlinearly related to the intraterminal Ca^{2+} concentration at the calyx of Held, and even minute changes in presynaptic Ca^{2+} influx can strongly influence release probability (Takahashi et al. 1996; Borst and Sakmann 1999). When $I_{\text{Ca(V)}}$ is elicited repetitively using brief AP-like depolarizations, the current amplitude can be augmented or reduced depending on the inter-stimulus interval and number of stimuli applied. The frequency dependence of this modulation has been studied in calyx (Taschenberger et al. 2002; Xu and Wu 2005; Nakamura et al. 2008) and endbulb (Lin et al. 2011) terminals by applying trains of depolarizations (typically 1 ms to 0 mV, Fig. 9.8). At the calyx of Held, $I_{\text{Ca(V)}}$ inactivation is observed at stimulus frequencies <20 Hz. Maximum current inactivation of about 15–20 % is observed at 5–10 Hz. At frequencies ≥ 50 Hz, $I_{\text{Ca(V)}}$ is initially enhanced (up to ~ 20 % for a frequency of 200 Hz) but thereafter declines (Xu and Wu 2005; Nakamura et al. 2008; Lin et al. 2011). The facilitation of the Ca^{2+} current may therefore contribute to synaptic facilitation, or it may counterbalance the processes leading to synaptic depression at high presynaptic discharge rates. During low frequency firing, Ca^{2+} current inactivation contributes significantly to synaptic depression at the young calyx of Held synapse (Xu and Wu 2005). Surprisingly, $I_{\text{Ca(V)}}$ inactivation is completely absent during trains of depolarizations at endbulb terminals (Fig. 9.8). Whereas robust facilitation of $I_{\text{Ca(V)}}$ is observed at frequencies ≥ 20 Hz, $I_{\text{Ca(V)}}$ remained stable throughout the train during low-frequency stimulation (1–10 Hz) (Lin et al. 2011).

9.9 Developmental Refinements

During early postnatal development, endbulb (Neises et al. 1982; Bellingham et al. 1998; Limb and Ryugo 2000) as well as calyx (Kandler and Friauf 1993; Chuhma and Ohmori 1998; Taschenberger and von Gersdorff 2000; Iwasaki and Takahashi 2001; Joshi and Wang 2002; Taschenberger et al. 2002, 2005) synapses

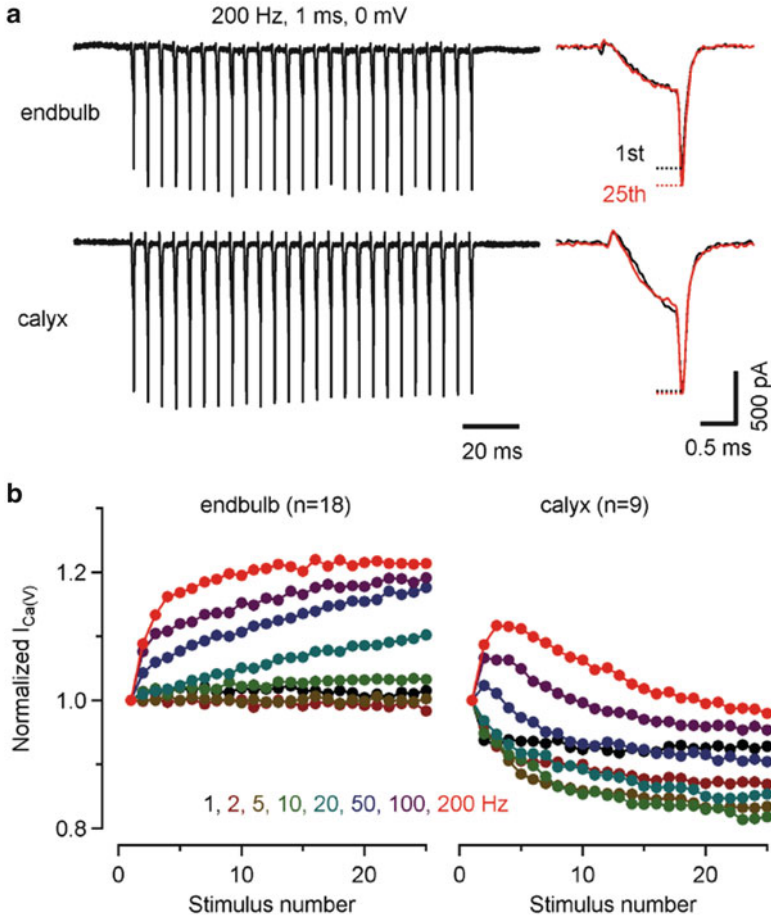


Fig. 9.8 Modulation of $I_{Ca(V)}$ during trains of AP-like depolarizations. (a) 200 Hz trains of $I_{Ca(V)}$ elicited by brief depolarizations (1 ms, 0 mV) recorded with a pipette solution containing 0.5 mM EGTA from an endbulb (*top*) and a calyx (*bottom*) terminal (*left panels*). Initial and final $I_{Ca(V)}$ are shown superimposed for comparison (*right panels*). Facilitation of $I_{Ca(V)}$ was observed during train stimulation of endbulb terminals. In calyx terminals, $I_{Ca(V)}$ inactivated after initial facilitation. (b) Modulation of presynaptic $I_{Ca(V)}$ during train stimulation at frequencies ranging from 1 to 200 Hz. Results from 18 endbulb (*left*) and nine calyx terminals (*right*) (Modified from Lin et al. 2011)

undergo several morphological and functional modifications which eventually transform them into fast and reliable relay synapses. Even though many of these developmental changes primarily affect the function of postsynaptic AMPA and NMDA receptor channels, a few prominent functional changes occur at the presynaptic site as well. Immature calyces express a mixture of N-, P/Q- and R-type VGCCs (Wu et al. 1998, 1999) whereas Ca^{2+} influx in more mature terminals predominantly depends on P/Q-type channels (Iwasaki and Takahashi 1998; Iwasaki et al. 2000).

It is possible that a similar developmental switch in the expression of $\alpha 1$ -subunits occurs at endbulb terminals as well. However, $I_{\text{Ca(V)}}$ in P9–11 endbulb terminals is already exclusively generated by P/Q-type VGCCs (Lin et al. 2011). Interestingly, in P/Q-type channel k.o. mice, $I_{\text{Ca(V)}}$ is reduced by less than 50 % at the calyx of Held. The contribution of N-type channels to $I_{\text{Ca(V)}}$ increases nearly tenfold and thus largely compensates for the lack of the $\text{Ca}_v2.1$ subunit (Inchauspe et al. 2004; Ishikawa et al. 2005). In addition, the activation curve obtained from tail currents shows a depolarizing shift in $\text{Ca}_v2.1$ -deficient compared to wildtype mice. This renders VGCCs less efficiently gated by the presynaptic AP waveform (Li et al. 2007) and, together with the lower Ca^{2+} channel density, is expected to cause a strongly reduced EPSC size. However, EPSC amplitudes in k.o. mice are surprisingly similar to those in wildtype mice (Ishikawa et al. 2005; Inchauspe et al. 2007). More importantly, facilitation of EPSCs, which is typically observed under low release probability conditions at wildtype synapses, is severely reduced in $\text{Ca}_v2.1$ -deficient mice. This suggests that EPSCs facilitation is mediated to a large degree by Ca^{2+} current facilitation (Inchauspe et al. 2004; Ishikawa et al. 2005; but see Müller et al. 2008).

In addition to changes in the pharmacological profile of presynaptic VGCCs, a consequential change of the presynaptic AP waveforms occurs at the calyx of Held, with more mature calyx terminals having significantly briefer and faster APs (Fig. 9.9a) (Taschenberger and von Gersdorff 2000; Nakamura and Takahashi 2007). Because the number of VGCCs increases only moderately during development (Fig. 9.9b), the shortening of the AP waveform causes a significant reduction of the presynaptic AP-evoked $I_{\text{Ca(V)}}$ (Fedchyshyn and Wang 2005) and may thereby contribute to the observed reduction of the release probability in more mature calyx synapses (Iwasaki and Takahashi 2001; Taschenberger et al. 2002). Interestingly, the reduced Ca^{2+} influx per AP is partially compensated by a tighter spatial coupling between VGCCs and docked vesicles as suggested by the following two observations: (I) The slow Ca^{2+} chelator EGTA is more effective in reducing glutamate release when dialyzed into young compared to more mature terminals (Fedchyshyn and Wang 2005) indicating a developmental shortening of the diffusional distance between synaptic vesicles and Ca^{2+} channels. (II) Significantly higher peak $[\text{Ca}^{2+}]_i$ concentrations are required when modeling AP-evoked release transients of more mature synapses (Wang et al. 2008; Kochubey et al. 2009). Apparently, this spatial reorganization of channel-vesicle coupling relies on the $\text{Ca}_v2.1$ Ca^{2+} channel subunit. VGCCs and docked vesicles appears to be less tightly coupled in the absence of P/Q-type Ca^{2+} channels because after pre-incubation with the membrane permeable chelator EGTA-AM glutamate release is more strongly attenuated in $\text{Ca}_v2.1$ -deficient compared to wildtype calyces (Inchauspe et al. 2007).

Immature calyx of Held terminals express a variety of G protein-coupled receptors (see above) some of which seem to be lost during synapse maturation. For example the inhibitory effects of 5-HT and adenosine are prominent in young terminals but become weaker during development, in parallel with a decrease in the A1 receptor immunoreactivity at the calyx terminal (Kimura et al. 2003; Mizutani et al. 2006). Similarly, the inhibition of EPSCs by mGluR agonists is strongly reduced in mature calyces (Renden et al. 2005). Moreover, the fraction

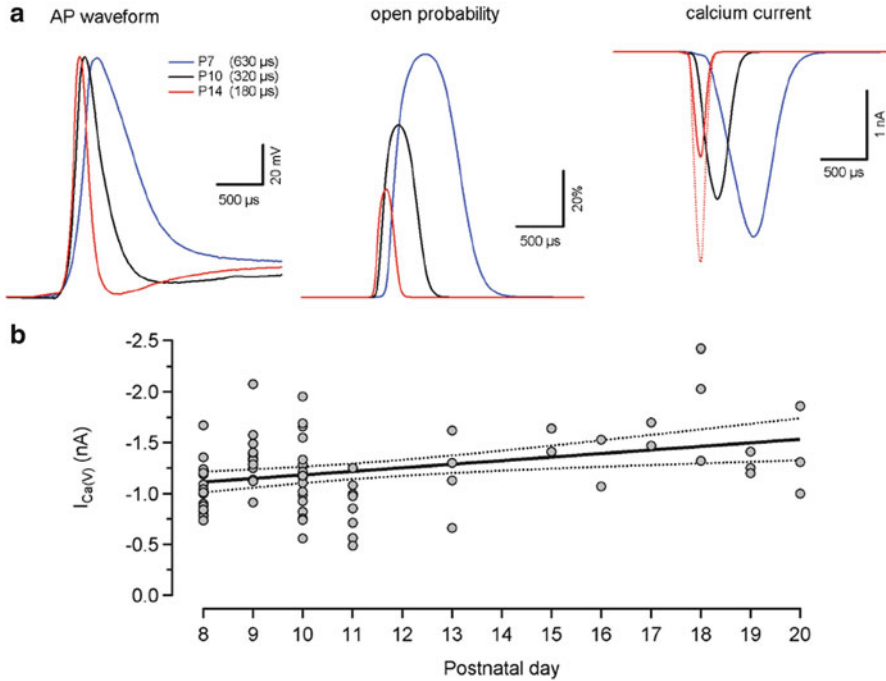


Fig. 9.9 Developmental changes in AP waveform and $I_{Ca(V)}$ at calyx terminals. **(a) Left:** Calyceal AP waveforms recorded at three different developmental stages. AP half-width is given in *parenthesis*. **Middle:** Corresponding time course of the activation parameter m^2 of a HH-model for $I_{Ca(V)}$ (Borst and Sakmann 1998b). Peak values were 88 %, 62 % and 39 % for the P7, P10 and P14 AP waveform, respectively. **Right:** Simulated AP-driven Ca^{2+} influx. Assuming equal Ca^{2+} channel densities at the three different ages, the predicted charge integrals were 1.4 pC, 0.6 pC and 0.2 pC. Note that even a doubling of the Ca^{2+} channel density at P14 (*red dotted line*) resulted in a significantly reduced AP-driven Ca^{2+} influx (0.4 pC) when compared to younger calyx terminals. **(b)** In mice calyces of Held, the amplitudes of $I_{Ca(V)}$ increase only slightly from P8 to P20. *Solid and dotted lines* represent linear regression and 95 % confidence intervals, respectively. The slope of the regression line is ~ 35 pA/day

of calyx synapses that are inhibited by noradrenaline strongly declines from 100 to ~ 25 % from P6 to P15, respectively, although the degree of inhibition does not change in responsive cells (Leao and von Gersdorff 2002). By contrast, activation of presynaptic GABA_B receptors strongly inhibits the EPSCs throughout development (Renden et al. 2005).

Relatively little is known about the role of presynaptic afferent activity for the maturation of calyx synapses. Presynaptic firing activity and neurotransmitter release may regulate synaptic strength (Turrigiano et al. 1998; Murthy et al. 2001; Thiagarajan et al. 2005) by modulating expression, trafficking, degradation and function of synaptic proteins (Rao and Craig 1997; O'Brien et al. 1998; Ehlers 2000; Townsend et al. 2004). Whereas the down regulation of postsynaptic NMDA receptor channels is significantly delayed in deaf mice und thus seems to be

controlled by afferent nerve activity, presynaptic Ca^{2+} influx and the transmitter release machinery appeared to be relatively insensitive to deprivation from afferent nerve activity (Futai et al. 2001; Youssoufian et al. 2005; Erazo-Fischer et al. 2007). In $\text{Ca}_v1.3^{-/-}$ deaf mice, presynaptic $I_{\text{Ca}(\text{V})}$ amplitudes were unaltered. The pharmacological profile of their presynaptic VGCCs was not tested, however Ca^{2+} current facilitation during high-frequency trains of AP-like depolarizations—which is the characteristic signature of calyceal P/Q-type VGCCs—is not different in deaf compared with wildtype mice.

9.10 Conclusions

Direct presynaptic patch-clamp recordings at endbulb and calyx synapses of the mammalian auditory brainstem have taught us valuable lessons about the physiology of presynaptic VGCCs at these terminals and these preparations will continue to be popular model synapses for examining the mechanisms of modulation of presynaptic Ca^{2+} influx. Much work is still ahead of us. A multitude of signaling molecules are involved in synaptic function and we have only begun to understand the machinery that orchestrates the molecular regulation of presynaptic Ca^{2+} channel function: presynaptic RIM scaffolding proteins are important for localizing Ca^{2+} channels to the active zone (Han et al. 2011) and the filamentous protein septin 5 participates in the developmental reorganization of VGCC to vesicle coupling (Yang et al. 2010). The fact that many conventional mouse knock out models are perinatally lethal has limited the usefulness of the calyx preparation for studying presynaptic function at the molecular level. However, Cre-lox based conditional knock out approaches (Han et al. 2011) and the use of viral vectors (Young and Neher 2009) may overcome these limitations in the future.

References

- Augustine GJ, Adler EM, Charlton MP (1991) The calcium signal for transmitter secretion from presynaptic nerve terminals. *Ann N Y Acad Sci* 635:365–381
- Barnes-Davies M, Forsythe ID (1995) Pre- and postsynaptic glutamate receptors at a giant excitatory synapse in rat auditory brainstem slices. *J Physiol* 488:387–406
- Bellingham MC, Lim R, Walmsley B (1998) Developmental changes in EPSC quantal size and quantal content at a central glutamatergic synapse in rat. *J Physiol* 511:861–869
- Billups B, Forsythe ID (2002) Presynaptic mitochondrial calcium sequestration influences transmission at mammalian central synapses. *J Neurosci* 22:5840–5847
- Borst JG, Sakmann B (1996) Calcium influx and transmitter release in a fast CNS synapse. *Nature* 383:431–434
- Borst JG, Sakmann B (1998a) Facilitation of presynaptic calcium currents in the rat brainstem. *J Physiol* 513:149–155
- Borst JG, Sakmann B (1998b) Calcium current during a single action potential in a large presynaptic terminal of the rat brainstem. *J Physiol* 506:143–157

- Borst JG, Sakmann B (1999) Effect of changes in action potential shape on calcium currents and transmitter release in a calyx-type synapse of the rat auditory brainstem. *Philos Trans R Soc B Biol Sci* 354:347–355
- Borst JG, Soria van Hoeve J (2012) The calyx of held synapse: from model synapse to auditory relay. *Annu Rev Physiol* 74:199–224
- Borst JG, Helmchen F, Sakmann B (1995) Pre- and postsynaptic whole-cell recordings in the medial nucleus of the trapezoid body of the rat. *J Physiol* 489:825–840
- Brawer JR, Morest DK (1975) Relations between auditory nerve endings and cell types in the cat's anteroventral cochlear nucleus seen with the Golgi method and Nomarski optics. *J Comp Neurol* 160:491–506
- Cavelier P, Hamann M, Rossi D, Mobbs P, Attwell D (2005) Tonic excitation and inhibition of neurons: ambient transmitter sources and computational consequences. *Prog Biophys Mol Biol* 87:3–16
- Chuhma N, Ohmori H (1998) Postnatal development of phase-locked high-fidelity synaptic transmission in the medial nucleus of the trapezoid body of the rat. *J Neurosci* 18:512–520
- Cuttle MF, Tsujimoto T, Forsythe ID, Takahashi T (1998) Facilitation of the presynaptic calcium current at an auditory synapse in rat brainstem. *J Physiol* 512:723–729
- DiGregorio DA, Peskoff A, Vergara JL (1999) Measurement of action potential-induced presynaptic calcium domains at a cultured neuromuscular junction. *J Neurosci* 19:7846–7859
- Ehlers MD (2000) Reinsertion or degradation of AMPA receptors determined by activity-dependent endocytic sorting. *Neuron* 28:511–525
- Erazo-Fischer E, Striessnig J, Taschenberger H (2007) The role of physiological afferent nerve activity during in vivo maturation of the calyx of held synapse. *J Neurosci* 27:1725–1737
- Fedchyshyn MJ, Wang LY (2005) Developmental transformation of the release modality at the calyx of held synapse. *J Neurosci* 25:4131–4140
- Forsythe ID (1994) Direct patch recording from identified presynaptic terminals mediating glutamatergic EPSCs in the rat CNS, in vitro. *J Physiol* 479:381–387
- Forsythe ID, Tsujimoto T, Barnes-Davies M, Cuttle MF, Takahashi T (1998) Inactivation of presynaptic calcium current contributes to synaptic depression at a fast central synapse. *Neuron* 20:797–807
- Futai K, Okada M, Matsuyama K, Takahashi T (2001) High-fidelity transmission acquired via a developmental decrease in NMDA receptor expression at an auditory synapse. *J Neurosci* 21:3342–3349
- Gillespie JJ (1979) The effect of repetitive stimulation on the passive electrical properties of the presynaptic terminal of the squid giant synapse. *Proc R Soc Lond B Biol Sci* 206:293–306
- Glykys J, Mody I (2007) Activation of GABA_A receptors: views from outside the synaptic cleft. *Neuron* 56:763–770
- Habets RL, Borst JG (2006) An increase in calcium influx contributes to post-tetanic Potentiation at the rat calyx of held synapse. *J Neurophysiol* 96:2868–2876
- Han Y, Kaeser PS, Sudhof TC, Schneggenburger R (2011) RIM determines Ca²⁺ channel density and vesicle docking at the presynaptic active zone. *Neuron* 69:304–316
- Harlow ML, Ress D, Stoschek A, Marshall RM, McMahan UJ (2001) The architecture of active zone material at the frog's neuromuscular junction. *Nature* 409:479–484
- Held H (1893) Die zentrale gehörlleitung. *Archiv für Anat Physiol Anat Abtheilung* 17:201–248
- Helmchen F, Borst JG, Sakmann B (1997) Calcium dynamics associated with a single action potential in a CNS presynaptic terminal. *Biophys J* 72:1458–1471
- Inchauspe CG, Martini FJ, Forsythe ID, Uchitel OD (2004) Functional compensation of P/Q by N-type channels blocks short-term plasticity at the calyx of held presynaptic terminal. *J Neurosci* 24:10379–10383
- Inchauspe CG, Forsythe ID, Uchitel OD (2007) Changes in synaptic transmission properties due to the expression of N-type calcium channels at the calyx of held synapse of mice lacking P/Q-type calcium channels. *J Physiol* 584:835–851
- Ishikawa T, Kaneko M, Shin HS, Takahashi T (2005) Presynaptic N-type and P/Q-type Ca²⁺ channels mediating synaptic transmission at the calyx of held of mice. *J Physiol* 568:199–209

- Iwasaki S, Takahashi T (1998) Developmental changes in calcium channel types mediating synaptic transmission in rat auditory brainstem. *J Physiol* 509:419–423
- Iwasaki S, Takahashi T (2001) Developmental regulation of transmitter release at the calyx of held in rat auditory brainstem. *J Physiol* 534:861–871
- Iwasaki S, Momiya A, Uchitel OD, Takahashi T (2000) Developmental changes in calcium channel types mediating central synaptic transmission. *J Neurosci* 20:59–65
- Jaffe LA, Hagiwara S, Kado RT (1978) The time course of cortical vesicle fusion in sea urchin eggs observed as membrane capacitance changes. *Dev Biol* 67:243–248
- Jones BE, Friedman L (1983) Atlas of catecholamine perikarya, varicosities and pathways in the brainstem of the cat. *J Comp Neurol* 215:382–396
- Joshi I, Wang LY (2002) Developmental profiles of glutamate receptors and synaptic transmission at a single synapse in the mouse auditory brainstem. *J Physiol* 540:861–873
- Kandler K, Friauf E (1993) Pre- and postnatal development of efferent connections of the cochlear nucleus in the rat. *J Comp Neurol* 328:161–184
- Kimura M, Saitoh N, Takahashi T (2003) Adenosine A₁ receptor-mediated presynaptic inhibition at the calyx of held of immature rats. *J Physiol* 553:415–426
- Kochubey O, Han Y, Schneggenburger R (2009) Developmental regulation of the intracellular Ca²⁺ sensitivity of vesicle fusion and Ca²⁺-secretion coupling at the rat calyx of held. *J Physiol* 587:3009–3023
- Korogod N, Lou X, Schneggenburger R (2005) Presynaptic Ca²⁺ requirements and developmental regulation of posttetanic potentiation at the calyx of held. *J Neurosci* 25:5127–5137
- Leao RM, von Gersdorff H (2002) Noradrenaline increases high-frequency firing at the calyx of held synapse during development by inhibiting glutamate release. *J Neurophysiol* 87:2297–2306
- Li L, Bischofberger J, Jonas P (2007) Differential gating and recruitment of P/Q-, N-, and R-type Ca²⁺ channels in hippocampal mossy fiber boutons. *J Neurosci* 27:13420–13429
- Limb CJ, Ryugo DK (2000) Development of primary axosomatic endings in the anteroventral cochlear nucleus of mice. *J Assoc Res Otolaryngol* 1:103–119
- Lin KH, Oleskevich S, Taschenberger H (2011) Presynaptic Ca²⁺ influx and vesicle exocytosis at the mouse endbulb of held: a comparison of two auditory nerve terminals. *J Physiol* 589:4301–4320
- Lin KH, Erazo-Fischer E, Taschenberger H (2012) Similar intracellular Ca²⁺ requirements for inactivation and facilitation of voltage-gated Ca²⁺ channels in a glutamatergic mammalian nerve terminal. *J Neurosci* 32:1261–1272
- Llinas R, Sugimori M, Silver RB (1992) Microdomains of high calcium concentration in a presynaptic terminal. *Science* 256:677–679
- Masterton B, Jane JA, Diamond IT (1967) Role of brainstem auditory structures in sound localization. I. Trapezoid body, superior olive, and lateral lemniscus. *J Neurophysiol* 30:341–359
- Meinrenken CJ, Borst JG, Sakmann B (2003) Local routes revisited: the space and time dependence of the Ca²⁺ signal for phasic transmitter release at the rat calyx of held. *J Physiol* 547:665–689
- Mizutani H, Hori T, Takahashi T (2006) 5-HT_{1B} Receptor-mediated presynaptic inhibition at the calyx of held of immature rats. *Eur J Neurosci* 24:1946–1954
- Morad M, Davies NW, Kaplan JH, Lux HD (1988) Inactivation and block of calcium channels by photo-released Ca²⁺ in dorsal root ganglion neurons. *Science* 241:842–844
- Morest DK (1968) The growth of synaptic endings in the mammalian brain: a study of the calyces of the trapezoid body. *Z Anat Entwicklungsgeschichte* 127:201–220
- Müller M, Felmy F, Schwaller B, Schneggenburger R (2007) Parvalbumin is a mobile presynaptic Ca²⁺ buffer in the calyx of held that accelerates the decay of Ca²⁺ and short-term facilitation. *J Neurosci* 27:2261–2271
- Müller M, Felmy F, Schneggenburger R (2008) A limited contribution of Ca²⁺ current facilitation to paired-pulse facilitation of transmitter release at the rat calyx of held. *J Physiol* 586:5503–5520

- Murthy VN, Schikorski T, Stevens CF, Zhu Y (2001) Inactivity produces increases in neurotransmitter release and synapse size. *Neuron* 32:673–682
- Nagwaney S, Harlow ML, Jung JH, Szule JA, Ress D, Xu J, Marshall RM, McMahan UJ (2009) Macromolecular connections of active zone material to docked synaptic vesicles and presynaptic membrane at neuromuscular junctions of mouse. *J Comp Neurol* 513:457–468
- Nakamura Y, Takahashi T (2007) Developmental changes in potassium currents at the rat calyx of held presynaptic terminal. *J Physiol* 581:1101–1112
- Nakamura T, Yamashita T, Saitoh N, Takahashi T (2008) Developmental changes in calcium/calmodulin-dependent inactivation of calcium currents at the rat calyx of held. *J Physiol* 586:2253–2261
- Neher E, Marty A (1982) Discrete changes of cell membrane capacitance observed under conditions of enhanced secretion in bovine adrenal chromaffin cells. *Proc Natl Acad Sci U S A* 79:6712–6716
- Neises GR, Mattox DE, Gulley RL (1982) The maturation of the end bulb of held in the rat anteroventral cochlear nucleus. *Anat Rec* 204:271–279
- Nicol MJ, Walmsley B (2002) Ultrastructural basis of synaptic transmission between endbulbs of held and bushy cells in the rat cochlear nucleus. *J Physiol* 539:713–723
- O'Brien RJ, Kamboj S, Ehlers MD, Rosen KR, Fischbach GD, Huganir RL (1998) Activity-dependent modulation of synaptic AMPA receptor accumulation. *Neuron* 21:1067–1078
- Oertel D (1999) The role of timing in the brain stem auditory nuclei of vertebrates. *Annu Rev Physiol* 61:497–519
- Ramón y Cajal S (1911) *Histologie du système nerveux de l'homme et des vertébrés*. Instituto Ramón y Cajal, Madrid
- Rao A, Craig AM (1997) Activity regulates the synaptic localization of the NMDA receptor in hippocampal neurons. *Neuron* 19:801–812
- Renden R, Taschenberger H, Puente N, Rusakov DA, Duvoisin R, Wang LY, Lehre KP, von Gersdorff H (2005) Glutamate transporter studies reveal the pruning of metabotropic glutamate receptors and absence of AMPA receptor desensitization at mature calyx of held synapses. *J Neurosci* 25:8482–8497
- Rhode WS, Greenberg S (1992) Physiology of the cochlear nuclei. In: Popper AN, Fay RR (eds) *The mammalian auditory pathway: neurophysiology*. Springer, New York, pp 94–152
- Roberts WM, Jacobs RA, Hudspeth AJ (1990) Colocalization of ion channels involved in frequency selectivity and synaptic transmission at presynaptic active zones of hair cells. *J Neurosci* 10:3664–3684
- Ryugo DK, Sento S (1991) Synaptic connections of the auditory nerve in cats: relationship between endbulbs of held and spherical bushy cells. *J Comp Neurol* 305:35–48
- Ryugo DK, Wu MM, Pongstaporn T (1996) Activity-related features of synapse morphology: a study of endbulbs of held. *J Comp Neurol* 365:141–158
- Ryugo DK, Pongstaporn T, Huchton DM, Niparko JK (1997) Ultrastructural analysis of primary endings in deaf white cats: morphologic alterations in endbulbs of held. *J Comp Neurol* 385:230–244
- Schneggenburger R, Forsythe ID (2006) The calyx of held. *Cell Tissue Res* 326:311–337
- Schneggenburger R, Sakaba T, Neher E (2002) Vesicle pools and short-term synaptic depression: lessons from a large synapse. *Trends Neurosci* 25:206–212
- Sheng J, He L, Zheng H, Xue L, Luo F, Shin W, Sun T, Kuner T, Yue DT, Wu LG (2012) Calcium-channel number critically influences synaptic strength and plasticity at the active zone. *Nat Neurosci* 15:998–1006
- Stanley EF (1993) Single calcium channels and acetylcholine release at a presynaptic nerve terminal. *Neuron* 11:1007–1011
- Sun JY, Wu LG (2001) Fast kinetics of exocytosis revealed by simultaneous measurements of presynaptic capacitance and postsynaptic currents at a central synapse. *Neuron* 30:171–182
- Takahashi T, Forsythe ID, Tsujimoto T, Barnes-Davies M, Onodera K (1996) Presynaptic calcium current modulation by a metabotropic glutamate receptor. *Science* 274:594–597

- Takahashi T, Kajikawa Y, Tsujimoto T (1998) G-protein-coupled modulation of presynaptic calcium currents and transmitter release by a GABAB receptor. *J Neurosci* 18:3138–3146
- Taschenberger H, von Gersdorff H (2000) Fine-tuning an auditory synapse for speed and fidelity: developmental changes in presynaptic waveform, EPSC kinetics, and synaptic plasticity. *J Neurosci* 20:9162–9173
- Taschenberger H, Leao RM, Rowland KC, Spirou GA, von Gersdorff H (2002) Optimizing synaptic architecture and efficiency for high-frequency transmission. *Neuron* 36:1127–1143
- Taschenberger H, Scheuss V, Neher E (2005) Release kinetics, quantal parameters and their modulation during short-term depression at a developing synapse in the rat CNS. *J Physiol* 568:513–537
- Thiagarajan TC, Lindskog M, Tsien RW (2005) Adaptation to synaptic inactivity in Hippocampal neurons. *Neuron* 47:725–737
- Townsend M, Liu Y, Constantine-Paton M (2004) Retina-driven dephosphorylation of the NR2A subunit correlates with faster NMDA receptor kinetics at developing retinocollicular synapses. *J Neurosci* 24:11098–11107
- Tsujimoto T, Jeromin A, Saitoh N, Roder JC, Takahashi T (2002) Neuronal calcium sensor 1 and activity-dependent facilitation of P/Q-type calcium currents at presynaptic nerve terminals. *Science* 295:2276–2279
- Turrigiano GG, Leslie KR, Desai NS, Rutherford LC, Nelson SB (1998) Activity-dependent scaling of quantal amplitude in neocortical neurons. *Nature* 391:892–896
- von Gersdorff H, Borst JG (2002) Short-term plasticity at the calyx of held. *Nat Rev Neurosci* 3:53–64
- von Gersdorff H, Schneggenburger R, Weis S, Neher E (1997) Presynaptic depression at a calyx synapse: the small contribution of metabotropic glutamate receptors. *J Neurosci* 17:8137–8146
- Wang LY, Neher E, Taschenberger H (2008) Synaptic vesicles in mature calyx of held synapses sense higher nanodomain calcium concentrations during action potential-evoked glutamate release. *J Neurosci* 28:14450–14458
- Westenbroek RE, Sakurai T, Elliott EM, Hell JW, Starr TV, Snutch TP, Catterall WA (1995) Immunochemical identification and subcellular distribution of the alpha 1A subunits of brain calcium channels. *J Neurosci* 15:6403–6418
- Wu LG, Borst JG, Sakmann B (1998) R-type Ca²⁺ currents evoke transmitter release at a rat central synapse. *Proc Natl Acad Sci U S A* 95:4720–4725
- Wu LG, Westenbroek RE, Borst JG, Catterall WA, Sakmann B (1999) Calcium channel types with distinct presynaptic localization couple differentially to transmitter release in single calyx-type synapses. *J Neurosci* 19:726–736
- Wynne B, Robertson D (1996) Localization of dopamine-beta-hydroxylase-like immunoreactivity in the superior olivary complex of the rat. *Audiol Neurotol* 1:54–64
- Xu J, Wu LG (2005) The decrease in the presynaptic calcium current is a major cause of short-term depression at a calyx-type synapse. *Neuron* 46:633–645
- Yang YM, Fedchyshyn MJ, Grande G, Aitoubah J, Tsang CW, Xie H, Ackerley CA, Trimble WS, Wang LY (2010) Septins regulate developmental switching from microdomain to nanodomain coupling of Ca²⁺ influx to neurotransmitter release at a central synapse. *Neuron* 67:100–115
- Yawo H (1999) Involvement of cGMP-dependent protein kinase in adrenergic Potentiation of transmitter release from the calyx-type presynaptic terminal. *J Neurosci* 19:5293–5300
- Yoshikami D, Bagabaldo Z, Olivera BM (1989) The inhibitory effects of omega-conotoxins on Ca channels and synapses. *Ann N Y Acad Sci* 560:230–248
- Young SM Jr, Neher E (2009) Synaptotagmin has an essential function in synaptic vesicle positioning for synchronous release in addition to its role as a calcium sensor. *Neuron* 63:482–496
- Young ED, Oertel D (2004) The cochlear nucleus. In: Shepherd GM (ed) *The synaptic organization of the brain*, 5th edn. Oxford University Press, Oxford
- Yousoufian M, Oleskevich S, Walmsley B (2005) Development of a robust central auditory synapse in congenital deafness. *J Neurophysiol* 94:3168–3180